

Supplementary Information

Uniaxial negative thermal expansion facilitated by weak host-guest interactions

Materials

The 18-crown-6 and nitromethane were purchased from Sigma-Aldrich. Methyl iodide was obtained from Merck. All chemical were used as received.

Synthesis

The methyl iodide solvate ($C_{12}H_{24}O_6 \cdot 2CH_3I$) was prepared from a concentrated solution of 18-crown-6 in neat methyl iodide. The solution was stirred for 2 hours at room temperature after which it was stored at ca. 5 °C for slow evaporation. Crystals were obtained after 5 days.

Single crystal X-ray diffraction

Single crystal X-ray diffraction data were collected using a Bruker APEX-II Quasar CCD area-detector diffractometer equipped with an Oxford Cryosystems 700Plus cryostat. A multilayer monochromator with MoK α radiation ($\lambda = 0.71073 \text{ \AA}$) from an Incoatec I μ S microsource was used.

Data reduction was carried out by means of the standard procedure using the Bruker software package SAINT2 and the absorption corrections and the correction of other systematic errors were performed using SADABS.3 The structures were solved by direct methods using SHELXS-97 and refined using SHELXL-97.4 X-Seed5 was used as the graphical interface for the SHELX program suite. Hydrogen atoms were placed in calculated positions using riding models.

Table S1: Crystallographic details for **18C6N**

Empirical formula	C ₁₂ H ₂₄ O ₆ .2CH ₃ NO ₂	C ₁₂ H ₂₄ O ₆ .2CH ₃ NO ₂	C ₁₂ H ₂₄ O ₆ .2CH ₃ NO ₂	C ₁₂ H ₂₄ O ₆ .2CH ₃ NO ₂
Formula weight	386.40	386.40	386.40	386.40
Temperature (K)	90(2)	120(2)	150(2)	180(2)
Wavelength (Å)	0.71073	0.71073	0.71073	0.71073
Crystal system	Monoclinic	Monoclinic	Monoclinic	Monoclinic
Space group	P 2 ₁ /n	P 2 ₁ /n	P 2 ₁ /n	P 2 ₁ /n
Unit cell dimensions (Å, °)	<i>a</i> = 9.3091(14)	<i>a</i> = 9.2976(13)	<i>a</i> = 9.2849(12)	<i>a</i> = 9.2668(13)
	<i>b</i> = 7.8112(12)	<i>b</i> = 7.8579(11)	<i>b</i> = 7.9079(10)	<i>b</i> = 7.9623(11)
	<i>c</i> = 13.619(2)	<i>c</i> = 13.6419(19)	<i>c</i> = 13.6739(18)	<i>c</i> = 13.7151(19)
	α = 90	α = 90	α = 90	α = 90
	β = 100.710(2)	β = 100.755(2)	β = 100.818(2)	β = 100.907(2)
	γ = 90	γ = 90	γ = 90	γ = 90
Volume (Å ³)	973.1(3)	979.2(2)	986.2(2)	993.7(2)
Z	2	2	2	2
Calculated density (g cm ⁻³)	1.319	1.311	1.301	1.291
Absorption coefficient (mm ⁻¹)	0.112	0.111	0.110	0.109
F ₀₀₀	416	416	416	416
Approx. crystal size (mm ³)	0.27 x 0.36 x 0.40	0.27 x 0.36 x 0.40	0.27 x 0.36 x 0.40	0.27 x 0.36 x 0.40
θ range for data collection (°)	2.5 to 28.4	2.5 to 28.4	2.5 to 29.8	2.5 to 28.3
Miller index ranges	-12 $\leq h \leq$ 12; -10 $\leq k \leq$ 10; -18 $\leq l \leq$ 18	-12 $\leq h \leq$ 12; -10 $\leq k \leq$ 10; -18 $\leq l \leq$ 18	-12 $\leq h \leq$ 12; -10 $\leq k \leq$ 10; -18 $\leq l \leq$ 18	-12 $\leq h \leq$ 12; -10 $\leq k \leq$ 10; -18 $\leq l \leq$ 18
Reflections collected	14088	14239	14663	14545
Independent reflections	2429 [R _{int} = 0.023]	2433 [R _{int} = 0.025]	2626 [R _{int} = 0.024]	2464 [R _{int} = 0.024]
Completeness to θ_{\max} (%)	99.8	99.5	93.8	99.7
Data / restraints / parameters	2429 / 0 / 119	2433 / 0 / 119	2626 / 0 / 119	2464 / 0 / 119
Goodness-of-fit on F ²	1.10	1.08	1.09	1.09
Final R indices [I > 2 σ (I)]	R1 = 0.0316; wR2 = 0.0845	R1 = 0.0333; wR2 = 0.0872	R1 = 0.0377; wR2 = 0.0965	R1 = 0.0406; wR2 = 0.1031
R indices (all data)	R1 = 0.0356; wR2 = 0.0872	R1 = 0.0382; wR2 = 0.0907	R1 = 0.0465; wR2 = 0.1017	R1 = 0.0492; wR2 = 0.1087
Largest diff. peak and hole (e Å ⁻³)	-0.27, 0.35	-0.22, 0.31	-0.23, 0.28	-0.23, 0.30

Table S1 continued: *Crystallographic details for 18C6N*

Empirical formula	C ₁₂ H ₂₄ O ₆ .2CH ₃ NO ₂	C ₁₂ H ₂₄ O ₆ .2CH ₃ NO ₂	C ₁₂ H ₂₄ O ₆ .2CH ₃ NO ₂	C ₁₂ H ₂₄ O ₆ .2CH ₃ NO ₂
Formula weight	386.40	386.40	386.40	386.40
Temperature (K)	210K	240K	260K	273K
Wavelength (Å)	0.71073	0.71073	0.71073	0.71073
Crystal system	Monoclinic	Monoclinic	Monoclinic	Monoclinic
Space group	P 2 ₁ /n	P 2 ₁ /n	P 2 ₁ /n	P 2 ₁ /n
Unit cell dimensions (Å, °)	<i>a</i> = 9.2363(13)	<i>a</i> = 9.1902(15)	<i>a</i> = 9.1488(15)	<i>a</i> = 9.1231(14)
	<i>b</i> = 8.0254(11)	<i>b</i> = 8.1108(13)	<i>b</i> = 8.1812(13)	<i>b</i> = 8.2311(13)
	<i>c</i> = 13.7678(19)	<i>c</i> = 13.853(2)	<i>c</i> = 13.928(2)	<i>c</i> = 13.982(2)
	α = 90	α = 90	α = 90	α = 90.00
	β = 101.054(2)	β = 101.313(2)	β = 101.529(2)	β = 101.676(2)
	γ = 90	γ = 90	γ = 90	γ = 90.00
Volume (Å ³)	1001.6(2)	1012.5(3)	1021.5(3)	1028.2(3)
Z	2	2	2	2
Calculated density (g cm ⁻³)	1.281	1.267	1.256	1.248
Absorption coefficient (mm ⁻¹)	0.109	0.107	0.107	0.106
F ₀₀₀	416	416	416	416
Approx. Crystal size (mm ³)	0.27 x 0.36 x 0.40	0.27 x 0.36 x 0.40	0.27 x 0.36 x 0.40	0.27 x 0.36 x 0.40
θ range for data collection (°)	2.5 to 28.3	2.5 to 28.3	2.5 to 28.3	2.5 to 28.3
Miller index ranges	-12 ≤ <i>h</i> ≤ 12; -10 ≤ <i>k</i> ≤ 10; -18 ≤ <i>l</i> ≤ 18	-12 ≤ <i>h</i> ≤ 12; -10 ≤ <i>k</i> ≤ 10; -18 ≤ <i>l</i> ≤ 18	-12 ≤ <i>h</i> ≤ 12; -10 ≤ <i>k</i> ≤ 10; -18 ≤ <i>l</i> ≤ 18	-11 ≤ <i>h</i> ≤ 11; -10 ≤ <i>k</i> ≤ 10; -18 ≤ <i>l</i> ≤ 18
Reflections collected	14646	14825	14870	15176
Independent reflections	2477 [R _{int} = 0.025]	2509 [R _{int} = 0.026]	2530, [R _{int} = 0.028]	2542, [R _{int} = 0.028]
Completeness to θ_{\max} (%)	99.4	99.5	99.5	99.3
Data / restraints / parameters	2477 / 0 / 119	2509 / 0 / 119	2530 / 0 / 119	2542 / 0 / 119
Goodness-of-fit on F ²	1.067	1.113	1.084	1.047
Final R indices [<i>I</i> > 2 σ (<i>I</i>)]	R1 = 0.0472; wR2 = 0.1224	R1 = 0.0604; wR2 = 0.1757	R1 = 0.0737; wR2 = 0.2245	R1 = 0.0823; wR2 = 0.2599
R indices (all data)	R1 = 0.0602; wR2 = 0.1311	R1 = 0.0821; wR2 = 0.1930	R1 = 0.1035; wR2 = 0.2492	R1 = 0.1167; wR2 = 0.2926
Largest diff. peak and hole (e Å ⁻³)	-0.28, 0.37	-0.33, 0.39	-0.36, 0.42	-0.34, 0.47

Table S2: *Crystallographic details for C₁₂H₂₄O₆.2CH₃I*

Empirical formula	C ₁₂ H ₂₄ O ₆ .2CH ₃ I	C ₁₂ H ₂₄ O ₆ .2CH ₃ I
Formula weight	548.18	548.18
Temperature (K)	90K	273K
Wavelength (Å)	0.71073	0.71073
Crystal system	Monoclinic	Monoclinic
Space group	P2 ₁ /n	P2 ₁ /n
Unit cell dimensions (Å, °)	$a = 8.9459(4)$ $b = 8.4921(3)$ $c = 14.2485(5)$ $\alpha = 90$ $\beta = 107.082(2)$ $\gamma = 90$	$a = 9.0683(3)$ $b = 8.6955(2)$ $c = 14.2945(5)$ $\alpha = 90$ $\beta = 106.751(2)$ $\gamma = 90$
Volume (Å ³)	1034.70(7)	1079.34(6)
Z	2	2
Calculated density (g cm ⁻³)	1.760	1.687
Absorption coefficient (mm ⁻¹)	3.061	2.934
F ₀₀₀	536	536
Approx. Crystal size (mm ³)	0.05 x 0.15 x 0.15	0.05 x 0.15 x 0.15
θ range for data collection (°)	2.4 to 28.3	2.4 to 28.3
Miller index ranges	$-7 \leq h \leq 11$; $-11 \leq k \leq 8$; $-18 \leq l \leq 18$	$-7 \leq h \leq 12$; $-11 \leq k \leq 8$; $-19 \leq l \leq 19$
Reflections collected	8100	8606
Independent reflections	2568 [R _{int} = 0.018]	2677 [R _{int} = 0.019]
Completeness to θ_{\max} (%)	99.9	99.6
Data / restraints / parameters	2568 / 0 / 101	2677 / 0 / 101
Goodness-of-fit on F ²	1.052	1.026
Final R indices [I > 2 σ (I)]	R1= 0.0154 wR2 = 0.0386	R1= 0.0353; wR2 = 0.0797
R indices (all data)	R1= 0.0165; wR2 = 0.0391	R1= 0.0512; wR2 = 0.0878
Largest diff. peak and hole (e Å ⁻³)	-0.48, 0.75	-0.80, 1.02

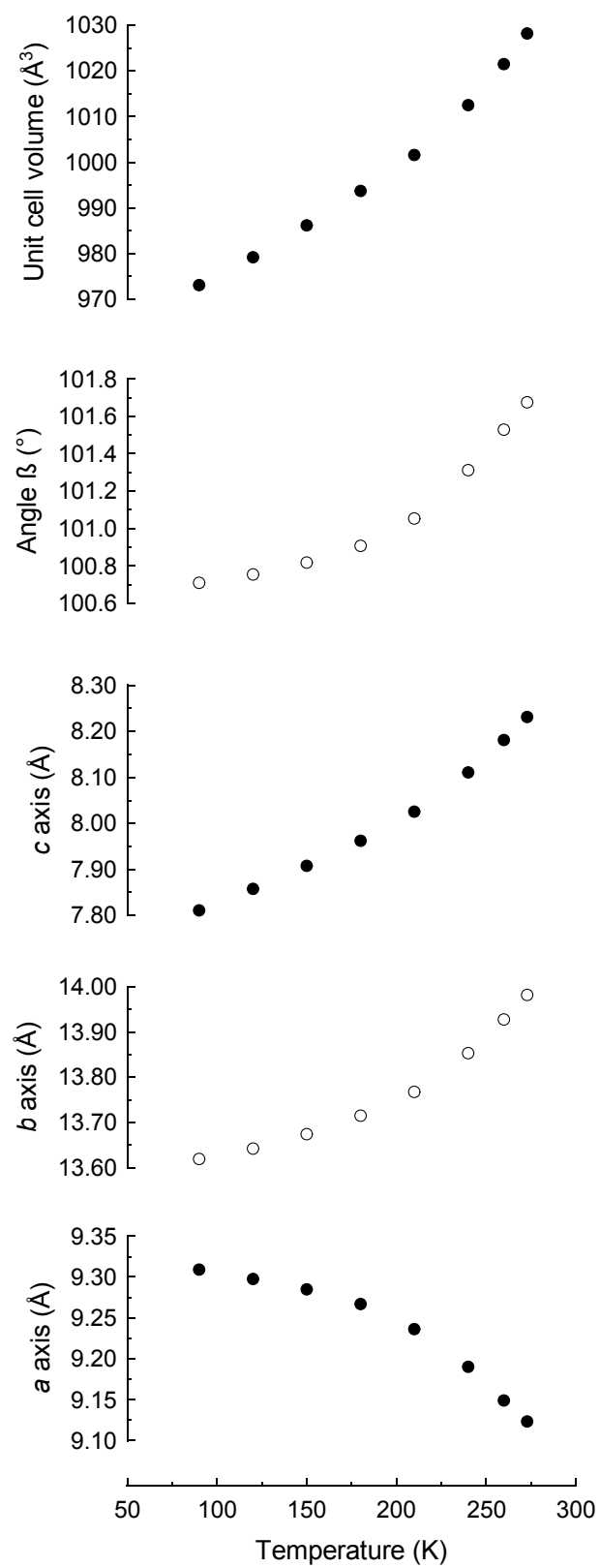


Figure S1: Unit cell dimensions and volume plotted against temperature in the range 90-273 K over which the same crystal was studied.

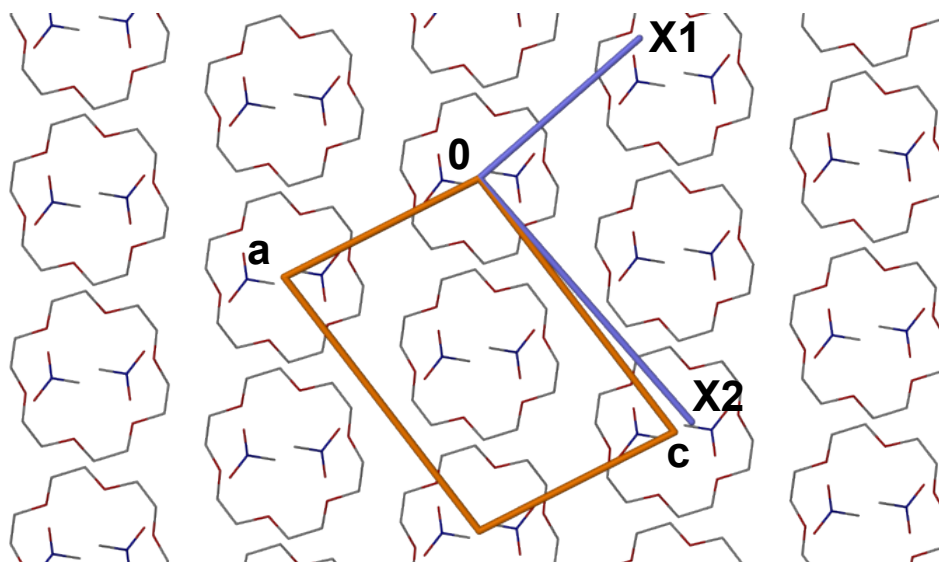


Figure S2: Orientation of $X1$ and $X2$ with respect to the crystallographic unit cell as viewed along $[0\ 1\ 0]$ (which is collinear with $X3$).

Cryogenic Powder X-ray Diffraction Powdered

Cryogenic powder X-ray diffraction samples were placed in a sealed glass capillary. X-ray powder diffractograms were measured using Cu $K\alpha$ radiation ($\lambda = 1.5418\ \text{\AA}$, 40 kV and 30 mA) on a PANalytical instrument operating in Bragg-Brentano geometry. The first diffractogram (2θ range from 5° to 40°) was measured at K, after which successive patterns were measured at 20 K intervals. The sample was cooled at a rate of $0.7\ \text{K min}^{-1}$ between measurements.

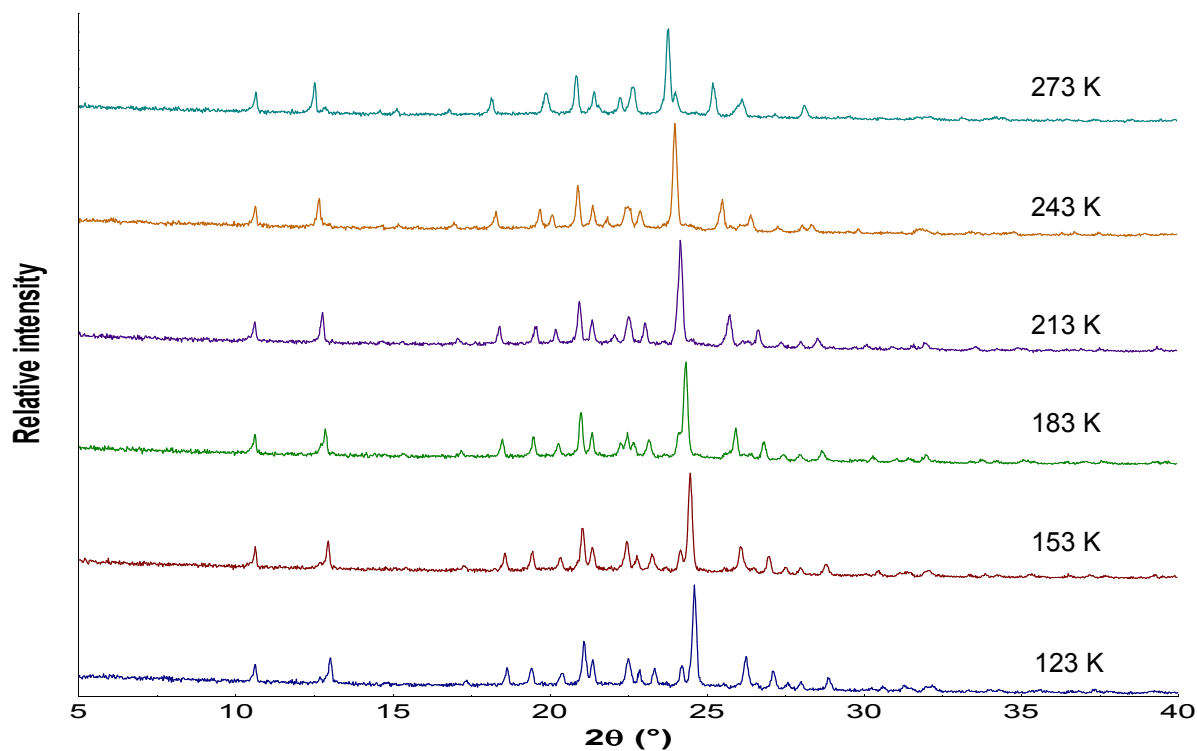


Figure S3: Temperature-resolved powder diffraction patterns for the same sample of $18C6N$ over the range 123K-273K.

Differential Scanning Calorimetry (DSC)

DSC experiments were carried out on a TA Instruments Q100 with Liquid Nitrogen Cooling Accessory (LNCS) and a Q20 with Refrigerated Cooling System (RCS90). The **18C6N** sample was cooled from 0 °C to -150 °C and subsequently heated to 0 °C at a rate of 5 °C/min. The nitromethane sample was cooled from 0 °C to -85 °C and subsequently heated to 0 °C at a rate of 5 °C/min.

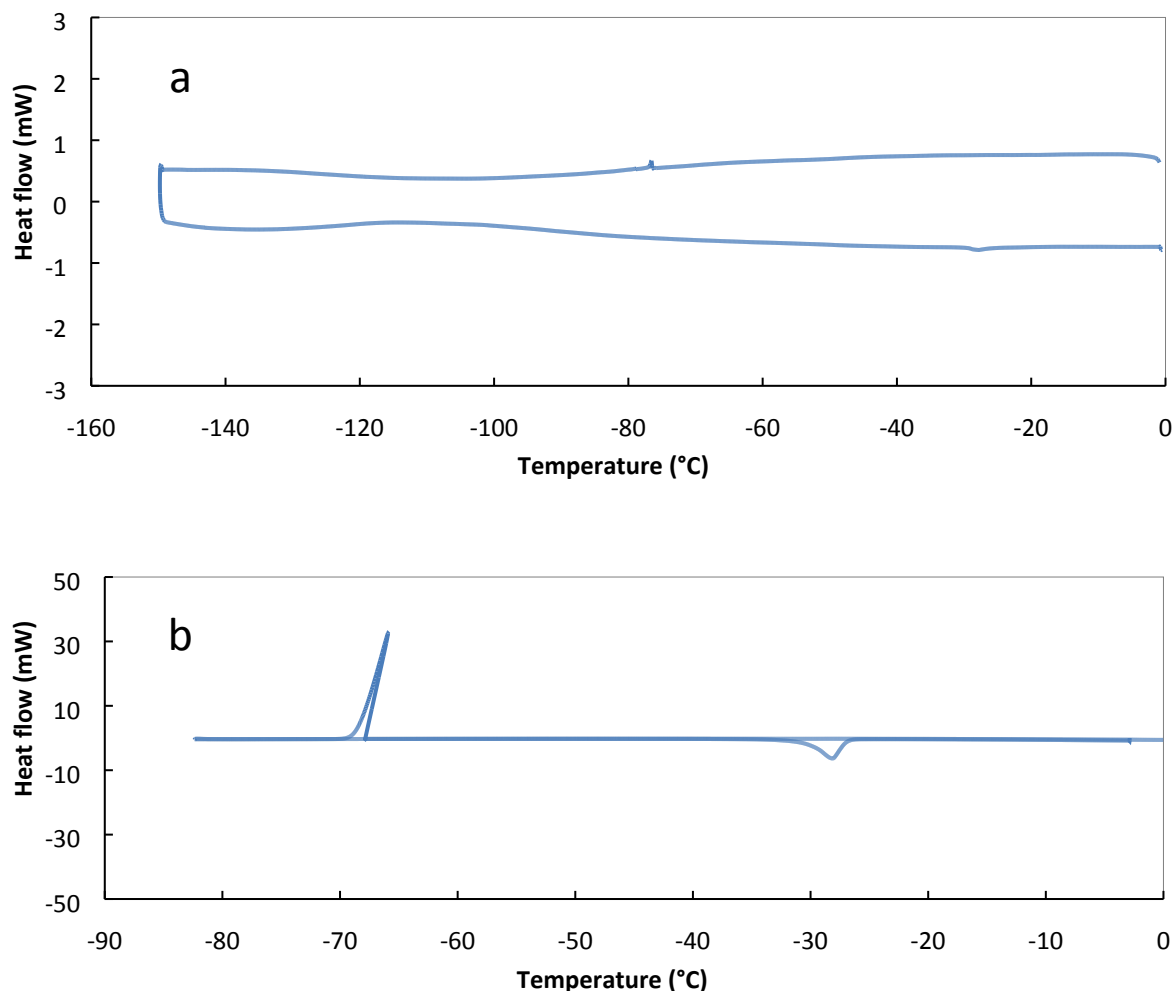


Figure S4: DSC curves for **18C6N** and neat nitromethane.

Computational

Atomic coordinates were imported from the refined crystal structures. Only the hydrogen atoms in the framework were optimized as part of a periodic system using the CASTEP module of the *Materials Studio* software suite.¹ The optimizations were performed using the GGA PBE functional with Grimme's DFT-D dispersion correction and thresholds for geometry optimization and SCF convergence were chosen as 1×10^{-5} and 1×10^{-6} eV respectively. The hydrogen optimized crystal structures were then used to determine H-bond angles (Figure S4). Single point energies calculations using the DMol3 module of the Materials Studio Software suite were performed using the GGA PBE functional with Grimme's DFT-D dispersion correction and threshold for SCF convergence were chosen as 1×10^{-6} eV. The electron density data obtained from the DMol3 calculations were used to construct the three dimensional 0.01 e-/Å³ electron density contour used for the molecular electrostatic potential map (obtained from the same calculation). The 18C6-guests and guest-guest interaction energies were calculated using DFT (Guassian09).² The hydrogen atoms which were fully optimized at the mPW1PW91/QZVP level of theory as well as the C-N and C-I bonds in nitromethane and iodomethane respectively. Although the change in bond length was small, it was required to achieve a geometry convergence.

Subsequent single point energies were performed at MP4/QZVP level of theory in order to determine the interaction energies.

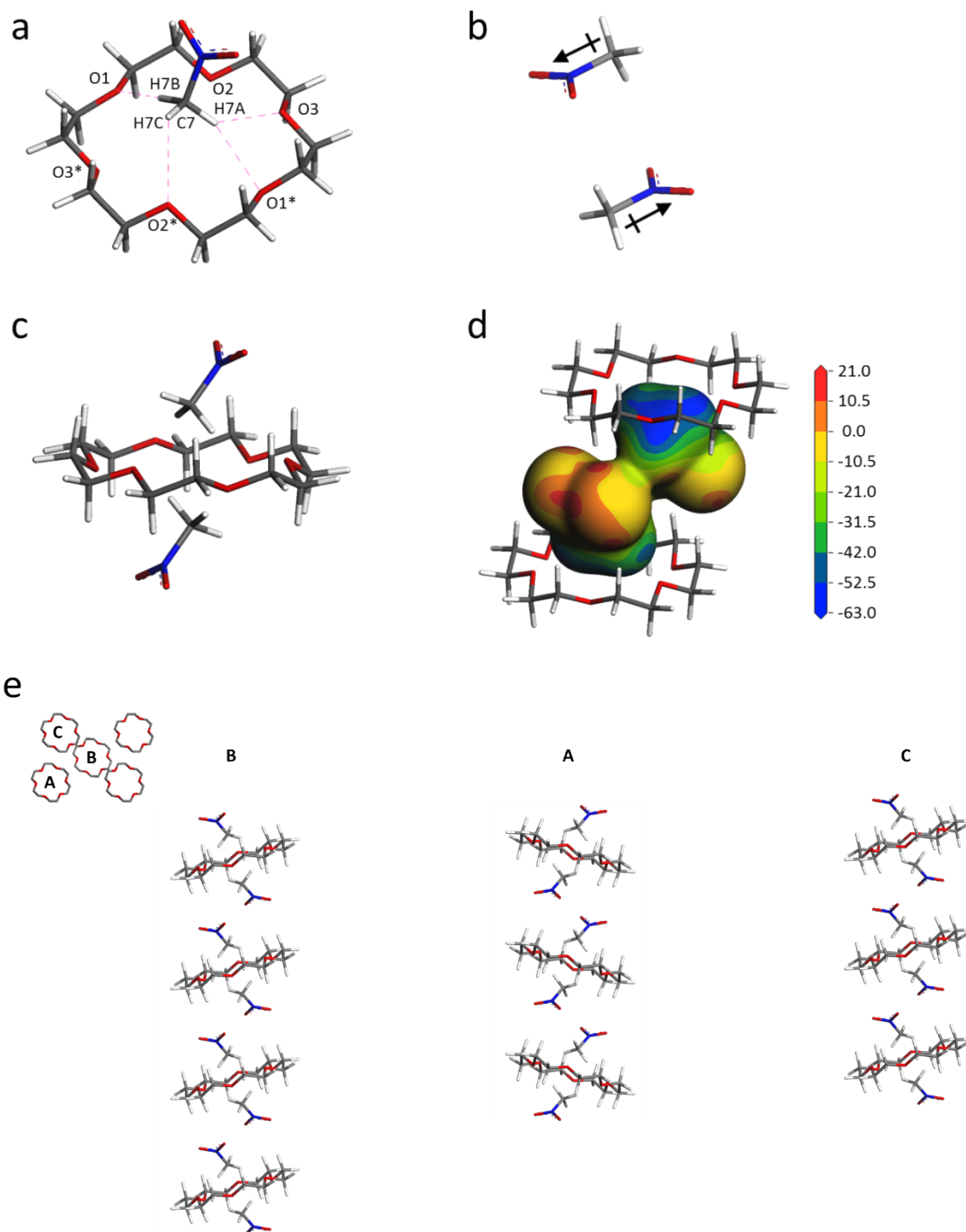


Figure S5: (a) The computational model used to determine the host-guest interaction energy. The dotted lines indicate the shortest C-H...O contacts. (b) The computational model used to determine the guest-guest interaction energy. (c) 1:2 host-guest adduct (d) The molecular electrostatic potential (MEP) of the host cavity is mapped onto a $0.01 \text{ e}^-/\text{\AA}^3$ electron density contour of the two guest molecules. The gradation on the scale bar is in kcal/mol with positive values in red and negative values in blue. (e) The computational models used for the MEP calculations of the host-guest columns with the column designations indicated.

Table S3: List of host-guest C–H \cdots O contacts for the 90K crystal structure of **18C6N** as determined after optimisation of hydrogen atom positions.

Contact	D \cdots A distance (Å)	D–H \cdots A angle (°)	273k distance	273k angle
C7–H7B \cdots O1	3.305(1)	175.4	3.274	168.1
C7–H7A \cdots O3	3.316(1)	135.8	3.325	152.5
C7–H7A \cdots O1*	3.505(1)	153.6	3.550	137.7
C7–H7B \cdots O2*	3.132(1)	106.8	3.231	122.3

Table S4: Distances and angles measured for the 90K and 273K crystal structures of **18C6N** after optimisation of hydrogen atom positions.

Parameter	90K	273K	Parameter change
O1–O1* distance (Å)	5.742	5.704	-0.038
O2–O2* distance (Å)	5.540	5.633	0.093
O3–O3* distance (Å)	5.778	5.718	-0.060
Host-guest distance (Å)	3.040	3.133	0.093
Host-host distance (adjacent along [0 1 0]) (Å)	7.811	8.231	0.420
Guest-guest distance (adjacent along [0 1 0]) (Å)	3.981	4.203	0.222
Torsion angle O4–N1–C7–H7 (°)	165.1	171.8	6.7

PASCal

PASCal calculations were carried out online at <http://pascal.chem.ox.ac.uk> using the Eulerian finite strain setting.

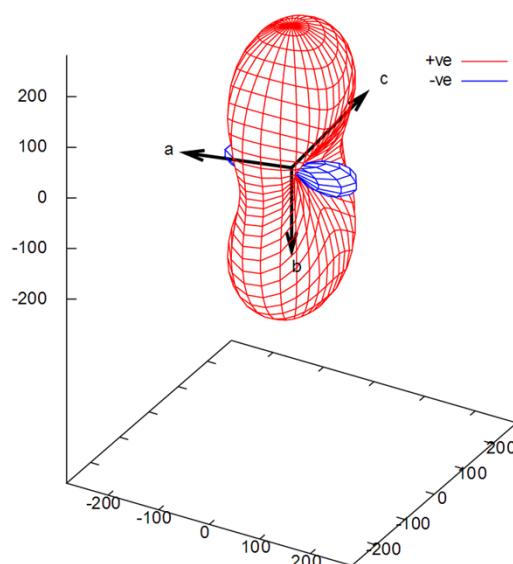


Figure S6: Expansivity indicatrix generated in PASCal.

Thermogravimetric analysis (TGA)

Thermogravimetric analysis was carried out using a TA Instruments Q500. The sample was heated at 10 °C/min from room temperature to decomposition. The experimental 32.5 % is in agreement with the expected 31.6 % based on single-crystal X-ray analysis.

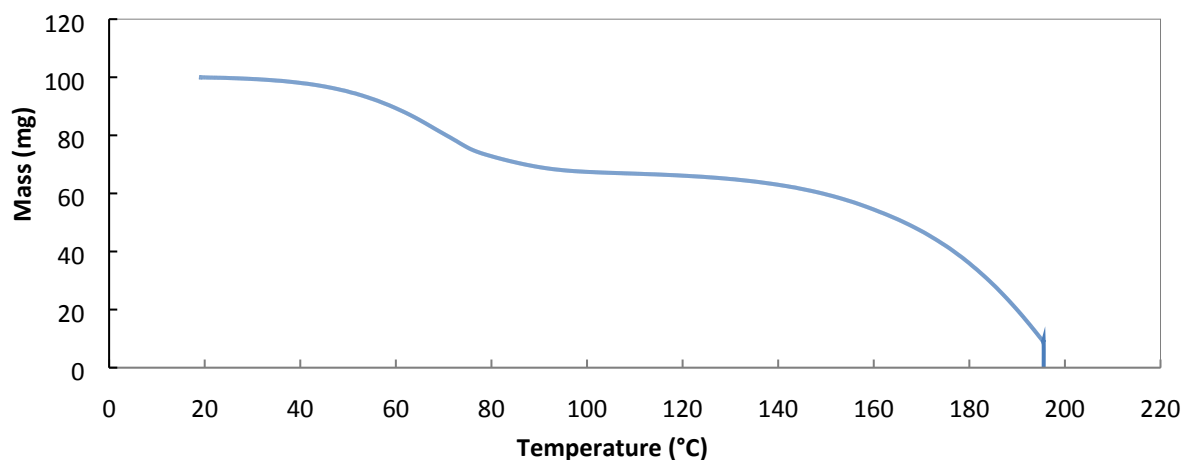


Figure S7: TGA curve for **18C6N**.

References

- 1 Materials Studio Modeling Environment (v6.0.0), Accelrys Software Inc., San Diego, 2011.
- 2 M. J. Frisch, G. W. Trucks, H. B. Schlegel, G. E. Scuseria, M. A. Robb, J. R. Cheeseman, G. Scalmani, V. Barone, B. Mennucci, G. A. Petersson, H. Nakatsuji, M. Caricato, X. Li, H. P. Hratchian, A. F. Izmaylov, J. Bloino, G. Zheng, J. L. Sonnenberg, M. Hada, M. Ehara, K. Toyota, R. Fukuda, J. Hasegawa, M. Ishida, T. Nakajima, Y. Honda, O. Kitao, H. Nakai, T. Vreven, J. A. Montgomery, Jr., J. E. Peralta, F. Ogliaro, M. Bearpark, J. J. Heyd, E. Brothers, K. N. Kudin, V. N. Staroverov, R. Kobayashi, J. Normand, K. Raghavachari, A. Rendell, J. C. Burant, S. S. Iyengar, J. Tomasi, M. Cossi, N. Rega, J. M. Millam, M. Klene, J. E. Knox, J. B. Cross, V. Bakken, C. Adamo, J. Jaramillo, R. Gomperts, R. E. Stratmann, O. Yazyev, A. J. Austin, R. Cammi, C. Pomelli, J. W. Ochterski, R. L. Martin, K. Morokuma, V. G. Zakrzewski, G. A. Voth, P. Salvador, J. J. Dannenberg, S. Dapprich, A. D. Daniels, Ö. Farkas, J. B. Foresman, J. V. Ortiz, J. Cioslowski, and D. J. Fox, Gaussian 09 (Revision B.01), Gaussian, Inc., Wallingford CT, 2009.